1 **Title:** The periaqueductal gray orchestrates sensory and motor circuits at multiple levels

2 of the neuraxis.

3

4 **Abbreviated title**: PAG control of sensorimotor systems

5

6 **Authors:** Stella Koutsikou[1,2*], Thomas C. Watson[1,3*], Jonathan J. Crook[1], J. Lianne

7 Leith[1], Charlotte L. Lawrenson[1], Richard Apps[1#], and Bridget M. Lumb[1#]

8

9 **Affiliations:** [1]School of Physiology, Pharmacology & Neuroscience, Medical Sciences

10 Building, University of Bristol BS8 1TD, UK. [2]School of Biological Sciences, Life

11 Sciences Building, University of Bristol BS8 1TQ, UK. [3]Neuroscience Paris Seine,

12 Cerebellum, Navigation & Memory Team, F-75005, Paris France (i) Sorbonne

13 Universities, UPMC University of Paris 06, UMR-S 8246; (ii) INSERM, UMR-S 1130;

14 (iii) CNRS, UMR 8246.

15 **Corresponding Author**

16 Professor Richard Apps

17 School of Physiology, Pharmacology & Neuroscience, Medical Sciences Building,

18 University of Bristol, University Walk, Bristol BS8 1TD

19 R.Apps@bristol.ac.uk

20 Tel: (+44) 117 3312264

21

22 **35 pages; 7 Figures; Words in Abstract: 217; Introduction: 499; Discussion: 1381**

23

24 **Conflict of Interest**: The authors declare no competing financial interests.

25

30

31 ***** SK & TCW share equal first authorship; [#]RA and BML are joint senior authors.

Abstract

The periaqueductal gray (PAG) co-ordinates behaviors essential to survival including striking changes in movement and posture (e.g. escape behaviors in response to noxious stimuli versus freezing in response to fear-evoking stimuli). However, the neural circuits underlying the expression of these behaviors remain poorly understood. We demonstrate *in vivo* in rats, that activation of the ventrolateral PAG (vlPAG) affects motor systems at multiple levels of the neuraxis: (i) through differential control of spinal neurons that forward sensory information to the cerebellum via spino-olivo-cerebellar pathways (nociceptive signals are reduced while proprioceptive signals are enhanced); (ii) by alterations in cerebellar nuclear output as revealed by changes in expression of Fos-like immunoreactivity; and (iii) through regulation of spinal reflex circuits, as shown by an increase in α-motoneuron excitability. The capacity to co-ordinate sensory and motor functions is demonstrated in awake behaving rats, in which natural activation of the vlPAG in fear conditioned animals reduced transmission in spino-olivo-cerebellar pathways during periods of freezing that were associated with increased muscle tone and hence motor outflow. The increase in spinal motor reflex excitability and reduction in transmission of ascending sensory signals via spino-olivo-cerebellar pathways occurred simultaneously. We suggest that the interactions revealed in the present study between the vlPAG and sensorimotor circuits could form the neural substrate for survival behaviors associated with vlPAG activation.

Significance Statement

Neural circuits that co-ordinate survival behaviors remain poorly understood. We demonstrate, in rats, that the periaqueductal grey (PAG) affects motor systems at multiple levels of the neuraxis: (i) through altering transmission in spino-olivary pathways that forward sensory signals to the cerebellum, reducing and enhancing transmission of nociceptive and proprioceptive information respectively; (ii) by alterations in cerebellar output; and (iii) through enhancement of spinal motor reflex pathways. The sensory and motor effects occurred at the same time and were present in both anesthetized animals, and in behavioural experiments in which fear conditioning naturally activated the PAG.

62   The results provide insights into the neural circuits that enable an animal to be ready and

63   able to react to danger, thus assisting in survival.

64

Introduction
65

66   The ability to interact with challenging environments requires detection of salient signals

67   that ultimately drive appropriate motor behaviors. These include defence behaviors such

68   as fear-evoked freezing which are dependent on the integrity of the periaqueductal gray

69   (PAG), and orchestrated by neurons in its ventrolateral sector (LeDoux et al., 1988;

70   Carrive et al., 1997; LeDoux, 2012). Neural substrates that underlie requisite alterations

71   in autonomic functions (e.g. cardio-respiratory adjustments) and sensory processing (e.g.

72   modulation of pain processing) that accompany defence are well understood (Lovick and

73   Bandler, 2005). However, little is known of the neural circuits that mediate the

74   characteristic motor responses associated with vlPAG activation.

75

76   We recently reported that activation of the vlPAG causes an increase in α-motoneuronal

77   excitability, which is thought to support freezing behavior (Koutsikou et al., 2014).

78   Defence behaviors also require that an animal's response is not perturbed from essential

79   motor activity, as would be caused by salient sensory information modifying activity in

80   supraspinal motor systems, leading to changes in behavior. Indeed, our initial

81   investigations (Cerminara et al., 2009) revealed that activation of the vlPAG can

82   significantly decrease cerebellar climbing fiber (CF) field potentials evoked by

83   stimulation of the hindlimb, indicating a reduction of CF activation by afferent systems.

84

85   CFs are generally thought to act as 'teaching' signals important for cerebellar cortical

86   plasticity (Ito, 2001). Reduction of transmission in ascending CF pathways might

87   therefore allow only behaviorally-relevant training signals to be forwarded to the

88   cerebellum. On the other hand, the timing hypothesis proposes that CFs have a more

89   direct influence on movement: their activation is thought to be capable of controlling

90   patterns of synchronous activity in the cerebellum that underlie motor coordination

91   (Llinas, 2011). In relation to the latter, our findings raise the possibility that the vlPAG

92   has the capacity to protect patterns of motor outflow in emergency situations by gating

93   distracting sensory inputs to cerebellar circuits that might otherwise perturb requisite

94   behavior.

95

96   To examine the nature and extent of modulatory influences of the vlPAG on different

97   qualities of sensory input to cerebellar circuits, the present study recorded spino-olivary

98   neurons, to determine any differential effects on innocuous (somatosensory and

99   proprioceptive) versus nociceptive transmission relayed via spino-olivo-cerebellar

100   pathways. Complementary functional anatomical studies also tested effects of the vlPAG

101   on nociceptor-evoked responses of cerebellar output circuits as assessed by the

102   expression of fos-like immunoreactivity in the cerebellar nuclei.

103

104   To examine effects of vlPAG modulation on spinal motor circuits, two further series of

105   experiments were carried out; one in anesthetised and one in awake animals, in which

106   effects of vlPAG activation were tested on spinal motor circuit excitability and freezing

107   behavior, respectively. An additional functionally pertinent question is whether localised

108   pools of neurons in the vlPAG control both motor outflow and sensory transmission at

109   the same time. To address this, spinal reflex and peripherally-evoked CF responses were

110   recorded simultaneously.

111

112   Overall, the results demonstrate that the vlPAG has the capacity to orchestrate processing

113   of sensory signals and motor output that together most likely underlie context-dependent

114   defensive responses, such as fear-evoked freezing behavior.

115

116   **Materials & Methods**

117   All animal procedures were performed in accordance with the UK Animals (Scientific

118   Procedures) Act 1986 and associated guidelines.

119   **Experiments in anesthetised animals**

120   *Recording of dorsal horn neuronal activity.* Experiments were carried out on 26

121   adult male Wistar rats weighing 290-320g and housed in standard conditions. Anesthesia

122   was induced with 2.5% halothane (Merial, UK) in O_2 and maintained by constant

123   intravenous (jugular vein) infusion of alphaxalone (30-40mg∕kg∕h; Vétoquinol, UK) and

124 maintained at a level at which there were no substantial changes in blood pressure

125 (measured via the carotid artery) in response to a firm pinch of the forepaw. The trachea

126 was cannulated to ensure patency of the respiratory tract and for artificial ventilation

127 when required. Arterial blood pressure and rectal temperature were monitored and

128 maintained within physiological limits. All animals were positioned in a stereotaxic

129 frame and a craniotomy was performed to allow access to the vlPAG (7.6-8.5mm caudal

130 from bregma, 0.8-1.0mm lateral to the midline, and ~5.3mm deep to the cortical surface,

131 (Paxinos and Watson, 2005).

132 A laminectomy was performed between T11-T13 to record from spinal dorsal

133 horn neurons in laminae I-V between lumbar segments L3-L5. The vertebral column was

134 clamped at each end of the laminectomy to increase stability during neuronal recordings.

135 The dura was removed from the surface of the spinal cord, a pool was made with the skin

136 flaps and the whole area was filled with warm agar. Once the agar was set a small

137 window was cut out over the desired recording site of the spinal cord and filled with

138 warm paraffin oil. A glass-coated tungsten micro-electrode (Merrill and Ainsworth,

139 1972) was lowered into the cord. Single-unit neuronal activity was amplified (x10k) and

140 filtered (500Hz-10kHz; NeuroLog System, Digitimer Ltd, UK) before being captured at

141 10k samples.s^{-1} via a 1401plus (CED, Cambridge UK) onto a PC running Spike2

142 software (CED, Cambridge UK).

143 *Antidromic testing of spinal neurons for a supraspinal projection.* Dorsal horn

144 neurons (*n* = 39 from 26 rats) were tested for a supraspinal projection to the caudal

145 brainstem. Supraspinal projection neurons were identified by their antidromic responses

146 to electrical stimulation in the vicinity of the contralateral inferior olivary complex (IO).

147 A craniotomy was performed to allow access to the contralateral inferior olive [~12.5

148 mm caudal to bregma, 1.2–1.5 mm lateral to the midline, and 8.5–9.0 mm deep to the

149 cortical surface according to the brain atlas of Paxinos and Watson (2005)], with a

150 bipolar stimulating electrode (interpolar distance of 0.5 mm; SNE-100X; Harvard

151 Apparatus). Single square pulses (20-100µA, 0.1ms duration at a rate of 0.1Hz) were

152 delivered via the stimulating electrode, and dorsal horn neurons were classified as

153 projection neurons if their action potentials met the following standard criteria for

154 antidromic activation (Fig 1*a*): (i) constant latency, (ii) frequency following to three

5

155   stimuli delivered at a rate of 200 Hz, and (iii) collision of the antidromic spike with a

156   spontaneous or evoked orthodromic spike (Fuller and Schlag, 1976; Lipski, 1981).

157   The possibility that electrical stimulation within the IO may have excited

158   ascending fibers that lie outside or course through the IO was minimised by positioning

159   the IO stimulating electrode at a depth where the minimum current was required to evoke

160   an antidromic spike (Fig. 1*b*). In support of this, Molinari and colleagues showed that

161   stimulus currents at a comparable intensity spread only minimally beyond the borders of

162   IO, and failed to activate axons of the medial lemniscus adjacent to the DAO (Molinari

163   and Dostrovsky, 1987). In the present study we aimed to confirm histologically as many

164   IO stimulation sites as possible (Fig. 1*d*). By adopting these approaches it therefore

165   seems reasonable to assume that the inferior olive was the main if not exclusive target of

166   spinal projection neurons identified in this study, and the term 'spino-olivary' is used

167   accordingly.

168   *Functional classification of spino-olivary neurons.* Once units were identified as

169   projecting to IO, the peripheral receptive field was characterised using natural mechanical

170   stimuli: low threshold (light brush, tap, gentle pressure, joint movement) and high

171   threshold (pinch with hand-held forceps). According to their response properties, the

172   spino-olivary units were classified into one of four groups as described by Menetrey et

173   al., (1977); class 1 (low threshold; innocuous), class 2 (low and high threshold; wide

174   dynamic range), class 3 (high threshold; nociceptive-specific) and class 4 (joint

175   movement and deep muscle pressure; proprioceptive). Responses to innocuous and

176   noxious stimuli were quantified by counting the total number of spikes evoked during

177   application of the stimulus and then subtracting spontaneous activity of the neuron,

178   measured for a similar time window prior to the stimulus.

179   *Neuronal activation of the ventrolateral PAG.* Glass micropipettes were advanced

180   into the caudal vlPAG under stereotaxic guidance (Paxinos and Watson, 2005).

181   Micropipettes were filled with 50mM of the excitatory amino acid DL-homocysteic acid

182   (DLH; Sigma) mixed with pontamine sky blue dye to mark the injection sites (McMullan

183   and Lumb, 2006a, b; Koutsikou et al., 2007). Pressure injections of DLH (60-80nl)

184   typically evoked decreases in mean arterial pressure. Subsequently, descending

185   influences from the vlPAG were tested: (i) on the responses of spino-olivary neurons to

186 natural peripheral stimulation; and (ii), in a different series of experiments, on H-reflex

187 and cerebellar field potential amplitudes (see detailed Methods below).

188 *Experimental protocol of descending modulation of spino-olivary neuronal*

189 *activity.* A pneumatic pincher was used to deliver mechanical stimuli (15s duration;

190 innocuous 0.5N and/or noxious 3.6N) every 5 minutes to the receptive fields of class 1-3

191 spino-olivary neurons. After three baseline responses were obtained from each unit, a

192 microinjection of DLH was made into the vlPAG, 5-10s prior to the onset of the next

193 pinch stimulus. Three additional cycles of pinch stimulation were then repeated to

194 monitor recovery from any descending influences. Only the last 10s of each response to

195 noxious pinch was analysed, as the initial 5s was presumed to contain a considerable

196 amount of low threshold rapidly adapting activity (Hartell and Headley, 1990). In this

197 and previous studies (McMullan and Lumb, 2006b; Leith et al., 2010), consistency of

198 responses indicate that repeated noxious stimuli (limited to 7 stimuli per animal) at 5

199 minute intervals does not result in tissue damage and/or hyperalgesia.

200 For responses evoked by innocuous mechanical stimuli only the first 5s of the

201 spike activity were analysed. Spontaneous activity, measured over 5-10s prior to the

202 onset of the stimulus, was subtracted from responses to noxious and innocuous stimuli

203 respectively. Responses of class 4 spino-olivary neurons were elicited by manual full

204 ankle joint rotation (Class 4 neurons did not fire in response to touch of the hind paw) of

205 the ipsilateral hindlimb for 10s every 3 minutes. After three baseline responses were

206 obtained, microinjection of DLH, was made into the vlPAG approximately 5-10s prior to

207 the onset of the next joint rotation/manipulation. The spike count of the entire 10s

208 duration response was corrected for spontaneous activity of the cell, measured over 10s

209 prior to the onset of the stimulus, and responses then analysed to test for any effects of

210 descending control.

211 *Histology.* At the end of every experiment positive DC current was applied

212 through the stimulating electrode to create lesions that were recovered post mortem to

213 establish electrode tip positions (Fig. 1*d*). Animals were killed with an overdose of

214 sodium pentobarbitone (i.v.) and following perfusion and fixation, the brain tissue was

215 removed and post-fixed for 24h in 4% phosphate-buffered paraformaldehyde solution.

216 The tissue was then transferred to 30% sucrose for at least 24h. Coronal sections (50μm)

217   of the midbrain and medulla were cut on a freezing microtome for histological

218   verification of pontamine sky blue injection sites and positioning of stimulating

219   electrodes in the PAG and IO, respectively.

220   *Fos immunohistochemistry.* Experiments were carried out on 32 adult male Wistar

221   rats weighing 250–350g. Anesthesia was induced using halothane (2.5% in O_2; Merial

222   UK) and, following preparatory surgery, was maintained by continuous intravenous

223   infusion of alfaxalone (30-40mg⁄kg⁄h; Vétoquinol, UK). Body temperature was monitored

224   and maintained at 37.0 ± 0.5^o C and venous, arterial and tracheal cannulations allowed

225   anesthetic administration, monitoring of arterial blood pressure and patency of the

226   respiratory tract respectively. In some experiments the head was fixed in a stereotaxic

227   frame (nose clamp and ear bars), and a small craniotomy performed to allow access to the

228   midbrain with glass pipettes. Following the preparatory surgery animals were allowed to

229   stabilize for a minimum period of 2h.

230   *Anesthetic control group.* Animals were cannulated and maintained as described

231   above for 4 hours. One anesthetic control group consisted of rats in which the jugular

232   vein, carotid artery and trachea were cannulated ($n = 4$). In a second anesthetic control

233   group ($n = 4$) only the jugular vein was cannulated. There was no significant difference

234   between these two groups (Kruskall-Wallis test), so the data were pooled ($n = 8$).

235   *PAG experimental group.* The PAG was chemically stimulated as described

236   above for the acute electrophysiological experiments. Changes (decreases) in blood

237   pressure evoked by the injection of DLH were recorded and helped to confirm that

238   injection sites were in the vlPAG. Saline control animals received an equivalent volume

239   of saline containing pontamine sky blue dye (60-80nl). Three injections of DLH ($n = 7$)

240   or saline ($n = 7$) were delivered at 10min intervals. The animals were then maintained

241   under anesthesia for a further 2h, timed from the second of the three injections, to allow

242   for expression of Fos protein in supraspinal structures (Koutsikou et al., 2007).

243   *Noxious pinch group.* In 6 alfaxalone anesthetised animals noxious stimuli were

244   applied to the snout using hand-held large rat-toothed forceps (3 x 20s pinches at

245   intervals of 10 minutes). Animals were then maintained under anesthesia for a further 2h

246   to allow time for the expression of Fos protein.

247   *Sodium nitroprusside group.* In 4 alfaxalone anesthetised animals, 3 intravenous

248   injections of sodium nitroprusside (100 ng/mL) were administered at intervals of 10

249   minutes. Animals were then maintained under anesthesia for a further 2h, timed from the

250   second injection, to allow time for the expression of Fos protein.

251   *Tissue processing.* At the end of every Fos experiment, animals were overdosed

252   with anesthetic and perfused as described previously for electrophysiological

253   experiments. Coronal sections (60μm) of the midbrain were cut, collected in 0.01M

254   phosphate buffer, mounted on gelatinised slides and then viewed under a Zeiss Axioskop

255   2+ Microscope. The injection sites were identified by the location of the dye spread and

256   pipette track, with reference to a stereotaxic atlas (Paxinos and Watson, 2005). Staining

257   for Fos-like immunoreactivity (FLI) in the cerebellum was carried out using previously

258   described methods (Koutsikou et al., 2007).

259   In brief, transverse sections (40μm) of cerebella embedded in gelatin were cut on

260   a freezing microtome. Every third section was processed free-floating for FLI using a

261   polyclonal rabbit Fos antibody (Santa Cruz Biotechnology; 1:5000 in 0.1M phosphate

262   buffer containing 1% bovine serum albumin, 0.1% triton X-100 and 0.01% sodium azide)

263   for 48–72 h at 4°C. Incubation in secondary biotinylated anti-rabbit antibody IgG (Sigma,

264   UK; 1:500 in 0.01M phosphate-buffered saline with 0.1% triton X-100 (PBS-T) was

265   carried out for 1–2 h at room temperature (20°C). The sections were subsequently

266   incubated in extravidin peroxidase (Sigma, UK; 1:1000 in PBS-T) for 1–2h and the

267   peroxidase visualized using 3,3-diaminobenzidine (0.015%; Sigma, UK) and glucose

268   oxidase (Sigma, UK). Finally, all sections were mounted onto gelatinised slides. A

269   number of sections from each series were processed in the absence of primary antibody,

270   in order to serve as negative controls.

271   *Fos-like immunoreactive microscopy and mapping.* Immunologically processed

272   sections were viewed under a 20X or 40X objective in order to identify FLI labelled cells.

273   Cells were counted as labelled if they displayed staining only in the nucleus, with a clear

274   contrast to the background staining in the immediate area (Hunt et al., 1987). A bright

275   nucleolus was often visible. FLI labelled cells were visually counted and mapped on to

276   standard coronal maps of the cerebellar nuclei adapted from Ruigrok and Voogd (1990,

277   2000). Since most FLI labelling was in the medial cerebellar nucleus (see Results),

278 quantitative analysis of FLI positive neurons was confined to its three subdivisions. No

279 difficulty was found in assigning cell labelling to the different subdivisions of the medial

280 nucleus on standard maps (Buisseret-Delmas, 1988; Buisseret-Delmas and Angaut,

281 1993). No significant differences in FLI were observed between ipsilateral and

282 contralateral regions in any of the groups ($P > 0.05$, Permutation paired t test, see

283 following section). FLI counts from cerebellar nuclear subdivisions on both sides were

284 therefore pooled for quantitative analysis.

285   Preliminary experiments sought to investigate the effects of vlPAG activation on

286 the inferior olive. However, in the absence of peripheral stimulation, background FLI in

287 the olive was highly variable and precluded reliable investigation of the effects of PAG

288 stimulation.

289   *Neuroanatomical statistical analysis.* In some cases, no FLI neurons were

290 observed in some subdivisions of the medial cerebellar nucleus. For this reason a

291 permutation one-way ANOVA, followed by post-hoc permutation t-tests with

292 Bonferroni's correction, was used to test for significant differences between groups. For

293 these statistical tests, the test statistic generated for the observed data is compared with

294 test statistics generated for random 'resampling' of the original data. A permutation P

295 value is calculated by observing the proportion of permutations that returned a test

296 statistic equal to or greater than the original test statistic. All permutation tests were based

297 upon 1,000,000 permutations (LaFleur and Greevy, 2009). Statistical analysis was carried

298 out with Rundom Pro v3.14. For all statistical tests the threshold for significance was

299 defined as $P < 0.05$.

300   *H-reflex recordings.* In 5 animals, a pair of stimulating needle electrodes (25G)

301 was inserted subcutaneously between the Achilles tendon and the distal tibial nerve of the

302 left hindlimb (Gozariu et al., 1998; Koutsikou et al., 2014). Constant current 50μs square

303 wave pulses were delivered at 3s intervals. A pair of intramuscular stainless steel

304 recording electrodes (0.075mm in diameter Teflon-coated; Advent Research Materials,

305 UK) was inserted into the ipsilateral plantaris muscle to record evoked EMG activity (M-

306 wave and H-reflex), in response to low intensity electrical stimulation of the nerve

307 (Mattsson et al., 1984; Gozariu et al., 1998).

308   The stimulus intensity was adjusted so that it was submaximal for evoking an H-

309   reflex response and the amplitude of the H-reflex was always larger than the M-wave.

310   The responses were amplified (x2k) and filtered (50Hz to 5kHz; Neurolog System,

311   Digitimer Ltd, UK) before being captured via a 1401plus A/D device (Cambridge

312   Electronic Design, CED, Cambridge UK). The individual H-reflex and M-wave peak-to-

313   peak amplitudes evoked by each stimulus were measured using Spike2 software (CED,

314   Cambridge UK). M-wave and H-reflex responses were recorded before and after

315   microinjection (60-80nl) of DLH (50mM; DLH, Sigma) into the vlPAG. The mean of 5

316   responses in each period: (i) prior: prePAG, (ii) immediately after: PAG, and (iii) 10min

317   after DLH microinjections: postPAG, were averaged and statistically compared to

318   determine any influence of the vlPAG on H-reflex amplitude. In all cases the H-reflex

319   data were normalised with respect to the M-wave. The latter serves as a useful internal

320   control of the constancy of the peripheral nerve stimulation. Note also that previous

321   studies have shown that the cerebellum does not have a tonic influence on H-reflex

322   excitability (Chen and Wolpaw, 2005).

323   *Recording of cerebellar cortical field potentials.* Simultaneous with recordings of

324   H-reflexes, in the same 5 rats described in the previous section, cerebellar field potentials

325   were recorded from the cortical surface of the copula pyramidis, following exposure of

326   the dorsal surface of the posterior lobe of the cerebellum. A low impedance silver wire

327   ball electrode was used to record extracellular field potentials in response to constant

328   current 50μs square wave pulses that were delivered at 3s intervals to the tibial nerve

329   (further details above). Cerebellar responses were recorded differentially between the ball

330   electrode and an indifferent (Ag-AgCl disc) placed in the bone margin lateral to the

331   cerebellar exposure. Responses were amplified and filtered (30Hz – 2.5kHz; Neurolog

332   System, Digitimer Ltd, UK), with any 50Hz electrical interference removed by a

333   Humbug device (QuestScientific, distributed by Digitimer Ltd, UK). The signal was

334   sampled at 20kHz using a CED 1401plus A/D converter (Cambridge Electronic Design,

335   UK) and recorded using Spike2 software (CED, UK). Responses were analysed offline:

336   the amplitude and latency to onset of the initial rising phase of individual evoked field

337   potentials was measured using Spike2 software.

338   *Experimental protocol to evoke simultaneous descending modulation of the H-*
339   *reflex and electrically-evoked cerebellar field potentials.* Peak-to-peak amplitude
340   measurements of M-wave (internal control), H-reflex and cerebellar field potentials were
341   made before and after microinjections of DLH into the vlPAG. The mean response (a)
342   prior (prePAG), (b) immediately after (PAG) and (c) 2 -10min after DLH (postPAG)
343   microinjection were averaged and statistically compared to determine any descending
344   influences on the peak-to-peak amplitudes.

345   *Histology.* At the end of every experiment animals were killed with an overdose
346   of sodium pentobarbitone (i.v.). The brains were removed and fixed for 24h in 4%
347   phosphate-buffered paraformaldehyde solution. The tissue was then transferred to 30%
348   sucrose for at least 24h. Coronal sections (50μm) of the midbrain were cut on a freezing
349   microtome for histological verification of pontamine sky blue injection sites in PAG.

350   **Experiments in awake animals**

351   *Implant Procedures.* Under sodium pentobarbital anesthesia (60mg/kg. I.P.) a
352   total of 14 adult male Wistar rats (300-400g, Charles River UK) were implanted with an
353   in-house built miniature microdrive, carrying up to 4 independently movable electrodes
354   (12.5μm tungsten wire, California Fine Wire, USA or 75um epoxy coated stainless steel,
355   FHC, Germany; impedance 100-200 kOhms at 1kHz). The microdrive was positioned
356   over the cerebellum (AP-12mm, ML 0.9mm relative from bregma). Optimal recording
357   position within the cerebellar cortex was determined by physiological recordings made
358   during surgery (to identify the cerebellar site where ipsilateral hindlimb stimulation
359   evoked the largest extracellular field potential; approximately 4mm from brain surface).
360   Pairs of flexible, stainless steel wires (Cooner Wire, USA) were sutured into the neck
361   muscles (Steenland and Zhuo, 2009) and used as EMG recording electrodes. Bipolar
362   stimulating wires (Cooner Wire, USA) were sutured subcutaneously within the hindlimb
363   (superficially and in close proximity to the ankle joint) ipsilateral to the cerebellar
364   recording electrodes. All leads were fed subcutaneously to connectors within the
365   headpiece (Pardoe et al., 2004). Post-surgery, animals were housed under normal
366   environmental conditions (~20°C and 45–65% humidity) on a 12 h dark–light cycle and
367   provided with food and water *ad libitum.*

368   *Awake animal recording.* Following recovery from surgery, differential

369 recordings were made using a Lynx 8 system (Neuralynx, Montana, USA), CED 1401

370 A/D device and Spike2 acquisition software (Cambridge Electronic Design, UK). A skull

371 screw above the cerebellum served as the reference for cerebellar field potential (CFP)

372 signals. EMG recordings from either side of the neck were referenced against each other

373 in a bipolar manner. Both EMG and CFP signals were sampled at 5kHz and filtered from

374 0.1Hz to 1kHz. Multi-unit activity was sampled at 25kHz and filtered from 300Hz to

375 6kHz. Video recordings were made throughout the experiments using a webcam (30

376 frames per second capture rate) and synchronised with electrophysiological data in

377 Spike2 software.

378   *Hindimb stimulation.* Electrical stimuli were applied via the peripherally

379 implanted stimulating wires (square pulses of 0.2ms duration; constant current). During

380 paired pulse experiments, stimuli were applied at varying time intervals (from 30 to

381 90ms). During fear tests, stimuli were typically applied every 1.5s at 1.5x the threshold

382 to evoke a CFP (Pardoe et al., 2004). This intensity of stimulus typically evoked a mild

383 twitch of the stimulated hindlimb but otherwise did not appear to disturb the animal.

384   *Fear conditioning.* Fear conditioning ($n = 5$) and testing for freezing (see below)

385 took place in two different contexts (A and B, respectively). The Skinner box (Med

386 Associates Inc., St Albans, VT, USA) and its floor were cleaned thoroughly with 70%

387 ethanol after every session. On days 1–3, animals were acclimatised for 5 min each day

388 to context A. On day 4, in context A, rats were exposed to an auditory cue (conditioned

389 stimulus, CS)–footshock (unconditioned stimulus, US; 0.75mA) fear-conditioned

390 protocol. This involved seven trials (30s inter-trial interval) of paired CS (1kHz auditory

391 tone, 75 dB, 10s duration) and US presentations (Sacchetti et al., 2004). Due to stimulus

392 and movement artefacts it was not possible to record electrophysiological responses

393 during fear conditioning.

394   *Fear–conditioned testing.* 24h after fear conditioning, each animal ($n = 5$) was

395 placed in the Skinner box with context B, and after 5min they were presented with 7×CS.

396 Freezing epochs were identified using a combination of neck EMG recordings

397 (Steenland and Zhuo, 2009), and video recordings. Freezing was confirmed by cessation

398 of all movements except those associated with respiration and eye movements and was

399   typically characterised by crouching postures (Blanchard and Blanchard, 1969). CFPs

400   were evoked at regular intervals (every 1.5s, see above) and neck EMG recorded

401   continuously throughout fear retrieval.

402   *Chemical Activation of vlPAG.* In one animal, a bilateral injection cannula

403   (Plastics One, USA) was implanted stereotaxically into the vlPAG (10° angle, AP -

404   2.2mm, ML 1mm from bregma, 5.5mm deep from brain surface). The vlPAG was

405   chemically activated using 100nl of 50mM DLH (Sigma, UK) containing pontamine sky

406   blue, which was pressure injected via the cannula whilst the animal was sitting quietly at

407   rest in its home cage. Evoked CFPs and neck EMG were recorded as indicated above,

408   before, during and after the DLH injection.

409   *Histology for chronic recording experiments.* At the end of each chronic

410   recording experiment, animals were overdosed and perfused as described above for

411   experiments in acutely anesthetised animals. Prior to perfusion, positive DC current was

412   applied through the recording electrodes to create lesions that were recovered post

413   mortem to establish electrode tip positions (Fig. 5). Cerebellar sagittal sections (50-

414   80μm) were processed in the same manner as for the non recovery experiments.

415   *Analysis.* Single unit neuronal activity, EMG and evoked CFP amplitudes were

416   displayed as mean ± s.e.m. Evoked CFPs were detected and measured (peak-to-trough

417   amplitude) using automated Spike2 scripts then averaged across stimulation trials. Due to

418   differences in field potential amplitude across animals (presumably due to variations in

419   recording site position), pooled data were normalized by expressing mean response

420   amplitude as a percentage of baseline amplitude. Freezing epochs were identified from

421   rectified and smoothed (0.025s) neck EMG recordings (Steenland and Zhuo, 2009) using

422   custom scripts in Spike2 software. Neck EMG amplitude was compared during fear

423   conditioning experiments by sampling (1 sample per second) the amplitude of rectified

424   and smoothed signal across the freezing and quiet rest epochs. Single unit activity was

425   sorted using Spike2 template matching and principle component algorithms.

426   *Electrophysiology statistical analysis.* All statistical analysis was performed using

427   Prism 5.0 (GraphPad, USA). Physiological recordings from awake animals were

428   statistically compared using paired or unpaired *t* tests, one-way ANOVA (with

429   Bonferroni's post-test) and repeated measures ANOVA (with Dunnett's post-test) tests as

430 appropriate. Responses following PAG activation were compared to pre and post PAG

431 responses using repeated measures ANOVA (with Dunnett's post-test). *P* values lower

432 than 0.05 were taken as statistically significant.

433

434 **Results**

435 *Characteristics of spino-olivary neurons.* Spino-olivary neurons were recorded in

436 order to study influences of the vlPAG on ascending projections that influence

437 supraspinal motor systems. Figs 1*a-c* illustrate the identification and properties of spino-

438 olivary neurons. Of our sample of dorsal horn neurons, 32 met all three standard criteria

439 for antidromic activation (see Methods) and were selected for further analysis.

440 *Descending modulation of spino-olivary neuronal responses to innocuous and/or*

441 *noxious stimuli.* All 32 dorsal horn neurons were classified by their responses to low and

442 high threshold mechanical stimulation of their receptive field area on the ipsilateral

443 hindleg (Fig. 1*c*), according to the scheme defined by Menetrey and colleagues

444 (Menetrey et al., 1977); class 1 (low threshold, $n = 2$), class 2 (wide dynamic range;

445 WDR, $n = 9$), class 3 (nociceptive specific, $n = 8$) and class 4 (proprioceptive, $n = 9$). In

446 addition, we recorded from spino-olivary projection neurons with unidentifiable receptive

447 fields ($n = 4$). Histological identification of stimulating electrode loci was possible for 19

448 cells. Figure 1*d* shows on standard transverse outlines of the inferior olive (Azizi and

449 Woodward, 1987) that the majority of stimulation sites were in the rostral dorsal

450 accessory olive (sites of antidromic activation of different classes of spino-olivary

451 neurons as follows: purple, class 1; green, class 2; red, class 3; and blue, class 4 cells).

452 To investigate descending control of sensory input to the olivocerebellar system,

453 including any selectivity, we examined the effects of activation of vlPAG on responses of

454 the different classes of spino-olivary projection neurons to noxious and non-noxious,

455 including proprioceptive, stimulation (total $n = 22$ neurons). The effects of neuronal

456 activation of vlPAG are illustrated as single examples and as pooled data in Figure 2.

457 Clear differences were evident between the effects of descending control on the

458 different classes of neurons with respect to effects on their responses to innocuous and

459 noxious stimuli, including responses to innocuous stimuli of different modality

460 (innocuous pressure *versus* proprioceptive). These can be summarised as follows: (i)

461 Class 2 neurons ($n = 7$); chemical stimulation in the vlPAG significantly reduced, by an

462 average of $51.6 \pm 8.9\%$, their noxious pinch-evoked response ($P = 0.011$, $F(2, 37) =$

463 5.15, repeated measures ANOVA followed by Dunnett's post test prePAG versus PAG;

464 Fig. 2*a*). In contrast, in three of the seven Class 2 neurons, vlPAG activation did not

465 significantly alter their response to low threshold innocuous pressure immediately

466 following PAG activation. Instead, a significant increase in the firing of these neurons

467 was observed 10-15min postPAG ($n = 3$, $P = 0.035$, $F(2, 18) = 4.06$, repeated measures

468 ANOVA followed by Dunnett's post test prePAG versus postPAG; Fig. 2*b*), (ii) Class 3

469 neurons ($n = 6$); chemical stimulation of vlPAG significantly reduced their response to

470 noxious pinch by an average of $94.1 \pm 4\%$ ($P = 0.0002$, $F(2, 22) = 13.04$, repeated

471 measures ANOVA followed by Dunnett's post test prePAG versus PAG; Fig. 2*c*). And

472 (iv), Class 4 neurons ($n = 8$); chemical excitation of vlPAG significantly increased their

473 response to joint movement, by an average of $96.1 \pm 23\%$ ($P < 0.0001$, $F(2, 52) = 13.23$,

474 repeated measures ANOVA followed by Dunnett's post test prePAG versus PAG; Fig.

475 2*d*), (v) Class 1 neurons; the response of a single class 1 spino-olivary neuron to

476 innocuous pressure (out of three identified) increased by 60% following chemical

477 stimulation of the vlPAG (Fig. 2*e*, not discussed further). Histologically recovered sites

478 of microinjection of DLH in the vlPAG are shown in Figure 2*f*.

479   The results of this first series of experiments therefore provide evidence that the

480 vlPAG influences supraspinal motor systems by differentially modulating sensory signals

481 of different modality that are forwarded to the cerebellum via ascending spino-olivary

482 projections. Transmission of nociceptive signals is reduced, while transmission of

483 proprioceptive signals is facilitated.

484   *Effects of vlPAG activation on Fos-expression in the cerebellar nuclei.* To

485 determine whether the vlPAG can influence cerebellar output we next assessed the effects

486 of vlPAG stimulation on activity in the cerebellar nuclei, the principal source of output

487 from the cerebellum. Initially, counts of Fos-like immunoreactive (FLI) neurons were

488 made in the cerebellar nuclei in two groups; animals mounted in a stereotaxic frame and

489 injected with either (i) saline or (ii) DLH into the vlPAG. The unexpected findings from

490 these initial experiments led us to carry out two additional groups of experiments in

491   which animals were not mounted in a stereotaxic frame: (iii) anesthetic controls and (iv)

492   animals pinched in the trigeminal domain (Fig. 3).

493   　　　Across all groups, the large majority of FLI neurons in the cerebellar nuclei (89.0

494   ± 10.7% of total) were located bilaterally in the medial cerebellar nucleus (MCN, in

495   regions related to cerebellar modules A, A2 and AX, n = 32). Since there were no

496   systematic differences between FLI labelling in the left and right hand cerebellar nuclei,

497   for simplicity only one side of the cerebellar nuclei is shown in Figure 3a. Statistically

498   significant differences were observed between groups i-iv and nitroprusside control

499   animals (n = 32) in the number of FLI neurons in regions of the cerebellar nuclei

500   associated with the A module (F$(4,27)$ = 3.46, $P < 0.05$, permutation one-way ANOVA).

501   and the A2 module (F$(4,27)$ = 2.86, $P < 0.05$), but not the AX module (F$4,27)$ = 1.32, P

502   > 0.05, see Fig. 4, the latter is not described further).

503   　　　Surprisingly, the initial experiments revealed that there were significantly more

504   FLI neurons in the A ($P > 0.05$, t = 2.2, df = 12 $post\text{-}hoc$ permutation t-test with

505   Bonferroni's correction) and A2 ($P > 0.05$, t = 2.4, df = 12) regions of MCN in animals

506   that received saline into the vlPAG (group (i), n = 7) compared with those injected with

507   DLH (group (ii), n = 7; Fig 3b). In both of these groups, animals were mounted in a

508   stereotaxic frame (with ear bars and a snout clamp), which raised the possibility that the

509   greater number of neurons in saline treated animals resulted from nociceptive inputs from

510   the trigeminal domain. To test this hypothesis two additional sets of experiments were

511   carried out in animals that were not mounted in a stereotaxic frame; anesthetic alone

512   controls, group (iii); and animals receiving a noxious stimulus in the trigeminal domain

513   (pinch of the snout) to mimic the stereotaxic procedure (group iv).

514   　　　Two observations support the view that the high levels of FLI in saline treated

515   animals did indeed arise from nociceptive input from the head and face: First, in both the

516   A and A2 regions of MCN there were no significant differences in numbers of FLI

517   neurons between saline injected and pinched animals (group (i) $versus$ group (iv), $P >$

518   0.05, t = 0.3 (A), t = 0.9 (A2), df = 11); and second, in both the A and A2 regions there

519   were significantly more FLI neurons in saline treated animals compared to anesthetic

520   controls (group (i) $versus$ group (iii), $P < 0.05$, t = 2.4 (A), t = 2.5 (A2), df = 11).

521   Further support is also provided by the tendency for there to be more FLI neurons in the

522   A region of MCN in animals that received noxious pinch of the snout when compared to

523   anesthetised control animals (group (iv) *versus* group (iii), mean $273\pm147\%$, $P = 0.057$, t

524    $= 2.56$, $df = 12$, *post-hoc* permutation t-test with Bonferroni's correction; Fig. 3*a-b*).

525   Taken together, we interpret these findings to indicate that the increased number

526   of FLI neurons in group (i) saline injected and group (iv) pinched animals, when

527   compared to group (iii) anesthetised controls that were not mounted in a stereotaxic head

528   holder, was due to nociceptive inputs from the trigeminal domain. If this is the case, then

529   the significant DLH-induced reduction of FLI neurons in the A and A2 module regions of

530   MCN ($n = 7$, A module region, mean $72\pm45\%$, A2 module region, mean $73\pm45\%$) when

531   compared to saline injected animals ($P < 0.05$, $t = 2.2$ (A), $t = 2.4$ (A2), $df = 12$, *post-hoc*

532   permutation t-test with Bonferroni's correction) most likely reflects a reduction in

533   nociceptor-evoked activity. It should be noted however that, although there was an

534   increase in numbers of FLI in the A2 module region in pinch when compared to

535   anesthetic controls, this difference was not statistically significant ($P > 0.05$, $t = 1.67$, *df*

536    $= 12$, *post-hoc* permutation t-test with Bonferroni's correction). This may reflect the

537   intensity of nociceptor stimulation that is required to activate significantly more neurons

538   in this particular module; stereotaxic procedures most likely evoke persistent/inescapable

539   nociceptive inputs when compared to pinch of the snout.

540   It would be of considerable interest to determine the effects of vlPAG activation

541   on responses in the cerebellar nuclei to proprioceptive stimulation. However, the design

542   of the Fos experiments precluded this as it would have been impossible to produce

543   reproducible synchronised peripheral stimulation and vlPAG stimulation, given (i) the

544   transient effects of PAG chemical stimulation and (ii) the nature of the peripheral

545   stimulus; manipulation of the limb.

546   In sum, the FLI data are consistent with effects of vlPAG action on cerebellar

547   outflow and in agreement with previous studies (Koutsikou et al., 2007), microinjections

548   of DLH into the vlPAG also produced a transient reduction in blood pressure (on average

549   by 16.2 ± 6.4 mmHg), whereas microinjections of saline did not produce any detectable

550   change. The locations of microinjections of DLH and saline into the vlPAG were

551   confirmed histologically (Fig. 3*c*). Two saline and 2 DLH cases were found to be within

552    $500\mu m$ of the lateral border of the vlPAG. However, injections of DLH from these

553   locations produced depressor effects that were indistinguishable to those evoked from

554   within the visible boundaries of the vlPAG.

555   The changes in blood pressure raise the possibility that the FLI results may be due

556   to autonomic effects. In 4 animals the effects of intravenous injection of sodium

557   nitroprusside were therefore also tested, at a dose (100 ng⁄mL) sufficient to mimic the

558   depressor effects of vlPAG stimulation. In every case this did not evoke significant

559   differences in the number of FLI cells in all regions of MCN, when compared to non-

560   surgical controls (Fig. 4*b*).

561   *Characterization of cerebellar field potentials in awake rats.* Having

562   demonstrated in anesthetised animals powerful differential effects of vlPAG activation on

563   the ability of spino-olivary pathways to relay sensory inputs of different modality to the

564   cerebellum; and on output from the cerebellar nuclei, we next sought to examine the

565   effect of natural PAG activation in a behavioral setting. To achieve this, we developed a

566   novel stimulation-recording technique that allowed us to monitor, in awake behaving rats,

567   peripherally evoked (hindlimb) cerebellar field potentials (CFPs) in the copula pyramidis

568   (COP, in the cerebellar cortical component of the C1 module, termed the C1 zone; Fig.

569   5*a-b*). We focussed our attention on transmission in spino-olivocerebellar paths that relay

570   information from hindlimb afferents to the cerebellar C1 zone because these paths

571   include direct spino-olivary projections that are thought to be especially concerned with

572   the modification of voluntary and reflex limb movements, and because there is extensive

573   knowledge of the anatomy and physiology of this particular cerebellar cortical zone in

574   rats (Atkins and Apps, 1997; Teune et al., 1998; Baker et al., 2001b; Pardoe and Apps,

575   2002; Pijpers et al., 2005; Ackerley et al., 2006; Pijpers et al., 2006).

576   Consistent with previous results in anesthetised rats (Atkins and Apps, 1997;

577   Cerminara et al., 2009) electrical stimulation of the ipsilateral hindlimb evoked robust

578   CFPs that were localised to specific recording sites within the cerebellar cortex (Fig. 5*a-*

579   *c*). Also, by simultaneously recording neck EMG, we were able to demonstrate that these

580   field potentials were not likely to be a far-field muscle response since they increased in

581   amplitude as a function of stimulation intensity that was independent of responses

582   detected in neck EMG. Evoked neck EMG activity was only observed when the stimulus

583   intensity was over 3 times the threshold (T) to evoke a detectable evoked cerebellar field

584 (for EMG: $P > 0.05$, $F(3, 27) = 0.90$; for CFPs: $P < 0.0001$, $F(3, 27) = 52.64$, repeated

585 measures ANOVA with Dunnett's post test versus baseline, $n = 7$ rats, Fig. 5d).

586   Consistent with previous studies (Atkins and Apps, 1997; Teune et al., 1998;

587 Jorntell et al., 2000; Baker et al., 2001a; Pardoe and Apps, 2002) individual cerebellar

588 recording sites were identified as being located within the hindlimb-receiving part of the

589 C1 zone in COP by their location in the medial part of the paravermal cortex and by the

590 presence of CFPs evoked by low intensity electrical stimulation of the ipsilateral

591 hindlimb (Fig. 5c). During implant surgery under sodium pentobarbital anesthesia the

592 onset latency of these CFPs was 16 ± 0.1ms with latency to peak of 19.5 ± 1.0ms ($n = 7$

593 rats). These latency measurements are in good agreement with previous studies in

594 anesthetised rats (Atkins and Apps, 1997). However, in the awake animal the onset

595 latency of responses recorded at the same recording sites consistently shifted significantly

596 earlier to an onset of 12.5 ± 0.1ms and peak of 15.9 ± 0.5ms, respectively; ($P < 0.001$, $t =$

597 5.8, $df = 6$, paired t test, $n = 7$ rats). No systematic difference was evident between onset

598 latency of individual CFPs and recording position in COP ($P > 0.05$, $F(2, 11) = 0.29$,

599 One-way ANOVA with Bonferroni's post-test, $n = 14$ rats).

600   The CFPs displayed the following features typical of climbing fiber field

601 potentials: (a) an onset latency that was always greater than 10ms (spino-cerebellar

602 mossy fiber responses have shorter latencies); (b) a highly characteristic waveform with a

603 duration of around 5ms that was always shorter than responses attributable to activity in

604 longer latency mossy fiber paths (Kennedy et al., 1966; Morissette and Bower, 1996); (c)

605 trial-by-trial fluctuations in response size; and (d) their pattern of response to a paired

606 pulse test was typical of climbing fiber responses. When two supramaximal stimuli were

607 delivered at interstimulus intervals ranging from 30 to 60 ms, the second response always

608 exhibited a reduction in size (Eccles et al., 1966; Armstrong and Harvey, 1968); $n = 7$

609 rats; red dashed line, Fig. 5e). An initial shorter latency response (presumably related to

610 mossy fiber inputs) was also sometimes present, which had an onset latency of $6.0 \pm$

611 0.3ms ($n = 14$). These earlier responses displayed no change in amplitude to a paired

612 pulse test and were not studied further (black dashed line, Fig. 5e).

613   Additional evidence that the longer latency CFPs were climbing fiber in origin

614 was obtained in 6 animals, in which we recorded single Purkinje cell activity at the same

615 cerebellar cortical recording sites where the largest field potentials were evoked. In every

616 case complex spike activity was evoked at a latency similar to that of the field potentials

617 (13.1 ± 1.4 ms; $n = 6$, Fig. 5f). Taken together, these data therefore suggest the longer

618 latency CFPs recorded in the awake animal were mainly climbing fiber in origin.

619 Having characterised the hindlimb evoked CFPs as mainly, if not exclusively,

620 climbing fiber in origin (and therefore relayed via spino-olivocerebellar paths, SOCPs)

621 we were in a position to examine the effect of artificial (DLH-evoked) and natural (fear-

622 evoked) activation of the vlPAG on their amplitude. Firstly, in one awake rat sitting

623 quietly at rest in its home cage, we injected DLH via an indwelling bilateral cannula to

624 chemically activate the vlPAG whilst electrically stimulating at regular intervals the

625 ipsilateral hindlimb at low intensity (1.5 x threshold for a detectable CFP; every 1.5s; see

626 methods for further details). As a result we were able to monitor any changes in CFP

627 amplitude and thus any modulation of SOCP transmission in the awake animal before,

628 during and after direct chemical activation of vlPAG neurons. Following injection of

629 DLH (dotted vertical line, Fig. 6a), the animal displayed a marked increase in freezing-

630 like behavior from a baseline of 50% at rest pre-DLH (indicated by the left hand light

631 gray horizontal bar in Fig. 6a) to 95% freezing-like behavior (indicated by the black bar

632 in Fig. 6a). Concomitant with the increase in freezing-like behavior, evoked CFPs

633 decreased in amplitude by about 30% (from 0.48 ± 0.02mV to 0.34 ± 0.01mV), then over

634 a period of about 500s, slowly returned to baseline levels as freezing-like behavior

635 subsided (0.49 ± 0.01mV; right hand light gray bar). Post mortem histology confirmed

636 the location of the cannulae within vlPAG (Fig. 6b).

637 *Climbing fiber fields are reduced during freezing behavior.* Whilst results

638 obtained from a single animal should be considered with caution, nonetheless these data

639 are proof of principle that SOCP transmission can be reduced by vlPAG activation in the

640 awake animal. This is in full agreement with more detailed analysis previously obtained

641 under anesthesia (Cerminara et al., 2009). As a result, we went on to examine the effects

642 on SOCP transmission of behaviorally more relevant activation of vlPAG. Using a fear-

643 conditioning paradigm, which is known to activate neurons in the vlPAG (Carrive et al.,

644 1997) we examined the effects on SOCP transmission during freezing (Fig. 6c). As

645 SOCPs are known to be gated during movement (Lidierth and Apps, 1990; Apps, 1999;

646   Apps and Lee, 1999; Apps, 2000) we restricted our comparison of evoked CFP amplitude

647   to periods of quiescence (animals at rest in their home cage displaying no movement),

648   and periods of conditioned freezing (in response to a previously conditioned auditory

649   tone, CS).

650   During CS evoked freezing, the amplitude of CFPs was moderately but

651   statistically significantly decreased compared to responses recorded during quiescence

652   (on average CFP amplitude reduced by 20 ± 2%, $P < 0.001$, $t = 8.8$, $df = 4$, paired t test, n

653   = 5; Fig. 6*c*). To identify freezing epochs we also recorded neck EMG during behavior

654   (Steenland and Zhuo, 2009). Concomitant with the decrease in CFP amplitude there was

655   also a tonic increase in neck EMG amplitude during freezing epochs compared to

656   quiescence (average increase of 25 ± 7 % $P < 0.05$, $t = 3.8$, $df = 4$, paired t test; $n = 5$

657   animals, Fig. 6*d*).

658   Taken together with our previous work (Cerminara et al., 2009; Koutsikou et al.,

659   2014) these results therefore suggest that, under certain conditions, vlPAG can both

660   decrease excitability in SOCPs and at the same time increase excitability in spinal motor

661   circuits. Given that similar phenomena would seem to be present in both awake and

662   anesthetised preparations, our final set of experiments explored whether this differential

663   modulation by the vlPAG can occur simultaneously.

664   *Simultaneous gating of SOCPs and modulation of motor outflow.* To determine

665   whether neurons in the vlPAG can simultaneously gate sensory transmission to

666   supraspinal motor systems (cerebellar evoked responses) and modulate spinal motor

667   outflow (α-motoneuron excitability), DLH was microinjected into the vlPAG of

668   anesthetized rats and recordings made simultaneously of CFP and spinal H-reflex

669   responses. Figure 7*a* illustrates typical examples of averaged raw data from a single

670   experiment. Low intensity electrical stimulation of the tibial nerve evoked CFPs in the

671   ipsilateral COP (C1 zone, Fig. 7a-*i*) and H-reflex responses in the ipsilateral hindlimb

672   (Fig. 7*a-ii*). In this case microinjection of DLH in vlPAG caused a transient abolition of

673   the CFP (prePAG *vs* PAG; Fig. 7*a-i***)**, whilst simultaneously increasing the amplitude of

674   the H-reflex response relative to baseline response size (prePAG *vs* PAG; Fig. 7*a-ii***)**. On

675   average, neuronal activation of vlPAG significantly decreased the amplitude of the CFP

676   by 89.8 ± 1% ($n = 5$, $P < 0.0001$, *F(2, 72)* = 92.46, repeated measures ANOVA followed

677 by Dunnett's post test versus prePAG; hatched bars, Fig. 7*b*), and significantly increased

678 the peak-to-peak amplitude of the H-reflex as indicated by an increase in the H:M ratio of

679 $38.8 \pm 0.4\%$ ($n = 5$, $P = 0.0025$, $F(2, 72) = 10.45$, repeated measures ANOVA followed

680 by Dunnett's post test versus prePAG; open bars, Fig. 7*b*). Both the CFP and H-reflex

681 responses returned to baseline levels within a 2-10min period following vlPAG

682 activation. Post-mortem histological reconstruction confirmed that the microinjections of

683 DLH were all located within vlPAG ($n = 5$, Fig. 7*c*). The effects of vlPAG on dorsal

684 horn neurons described above may affect motoneuronal output at a spinal segmental

685 level. For example, projection neurons in the dorsal horn which may be subject to

686 descending control have been shown to have collateral projections to the ventral horn

687 (Szucs et al., 2010). Nonetheless, these additional experiments still provide strong

688 evidence that vlPAG can orchestrate differential changes in ascending sensorimotor

689 projections and spinal motor systems simultaneously.

690

Discussion

691 **Discussion**

692 Despite the fundamental importance of motor behaviors evoked from the PAG, including

693 freezing co-ordinated by its ventrolateral sector, virtually nothing is known of the

694 underlying neural pathways and mechanisms. The current study has provided novel

695 insights into this issue. Importantly, we show that modulation of α-motoneuronal output

696 and fear-evoked freezing behavior can occur simultaneously with modulation of SOCPs,

697 presumably in a co-ordinated way and perhaps reflecting a common spinal mechanism.

698 *Effects of vlPAG on spinal processing in pre-cerebellar pathways:* This is the first

699 description in the rat of the physiological characteristics of spino-olivary neurons. As

700 detailed in the Methods, neurons were classified by their responses to cutaneous (noxious

701 and non-noxious) and proprioceptive inputs (limb manipulation). The proportions of

702 spino-olivary neurons in each class are similar to those described for unidentified (non-

703 projection) deep dorsal horn neurons (Waters and Lumb, 1997; McMullan and Lumb,

704 2006b; Waters and Lumb, 2008), including cells of origin of the spinothalamic tract

705 (Chung et al., 1979). Spino-olivary projections are relayed via the ventral funiculus

706 SOCP which involves a number of sub-paths that target cerebellar modules including the

707 A, A2 and AX zones in the vermis and the hindlimb C1 zone in the paravermis

708 (Oscarsson and Sjolund, 1977). The present characterization of dorsal horn activity and
709 evoked CFPs in response to vlPAG activation therefore included transmission in the same
710 general category of ascending pathways. These paths are thought to forward information
711 to the cerebellum about activity in segmental reflex circuits. In terms of projections to the
712 A modules such signals are presumably concerned with the control of balance and the
713 postural base for voluntary movements, including eye and head movements (Cerminara
714 and Apps, 2011); while signals forwarded to the hindlimb component of the C1 module
715 may be involved in the adaptive control of peripherally evoked reflexes during
716 locomotion (Lidierth and Apps, 1990; Apps et al., 1995; Pijpers et al., 2008).

717   Our dorsal horn recordings of spino-olivary projection neurons provide evidence
718 that descending control arising from the PAG selectively reduces transmission in spino-
719 olivary paths of acutely generated nociceptive signals. This selective control of cutaneous
720 input is consistent with previous studies of descending control of dorsal horn cells
721 (Heinricher et al., 2009), including those that project supraspinally such as spinothalamic
722 tract neurons. This raises the possibility that the spino-olivary tract may consist, at least
723 in part, of collaterals of the spinothalamic tract. However there is no direct evidence for
724 this and our previous anatomical pathway tracing studies indicate that this is unlikely to
725 be the case (Flavell et al., 2014).

726   Our dorsal horn recordings also found that transmission of non-noxious,
727 proprioceptive (presumably mainly group I afferent) signals is enhanced - a novel finding
728 with important implications. From a behavioral perspective it has been proposed that, in
729 active and passive defence scenarios, when the PAG is engaged, such selectivity would
730 depress nociceptive input that could distract an animal from carrying out behaviors
731 necessary for survival, and leave intact non-noxious information that provides precise
732 information with the capacity to direct motor activity to promote survival (Lumb, 2004).
733 We have reported previously that descending control of spinal transmission of non-
734 nociceptive information of cutaneous origin may be facilitated by the PAG (Waters and
735 Lumb, 2008) and other sites (Workman and Lumb, 1997; Simpson et al., 2008). Our
736 finding that vlPAG can also facilitate proprioceptive input to pre-cerebellar pathways
737 provides a mechanism whereby information from spinal circuits involved in monitoring
738 limb position and movement can be enhanced so refining sensory input that directs motor

739 control. Such an effect is entirely consistent with a role for the PAG in co-ordinating

740 motor behaviors in defence situations.

741   However, enhancement of transmission of proprioceptive signals via spino-

742 olivary projections would seem to conflict with our additional finding that transmission

743 of low threshold sensory signals is reduced in SOCPs targeting the hindlimb C1 zone in

744 COP. This apparent discrepancy may be explained by previous studies in decerebrate and

745 pentobarbitone anesthetised cats who reported that transmission of group I proprioceptive

746 signals in SOCPs arising from hindlimb nerves is weak and arises from specific

747 ipsilateral hindlimb nerves, notably quadriceps and gastrocnemus-soleus nerves, and is

748 relayed only when these nerves are repetitively stimulated (Armstrong et al., 1968;

749 Oscarsson, 1968). The stimulus location and parameters used in the present experiments

750 to electrically evoke activity in SOCPs may therefore have been insufficient to activate

751 group I afferents relayed via this route. Also, whilst considerable convergence from

752 nerves subserving different modalities is a consistent feature of the climbing fiber system,

753 nonetheless, cerebellar zones can differ in their pattern of afferent input. For example, the

754 C1 zone receives nociceptive cutaneous afferents while the neighbouring C2 zone does

755 not (Garwicz et al., 1992). This raises the possibility that proprioceptive afferents are

756 directed to specific parts of the cerebellar cortex not studied in the present experiments

757 (e.g. hindlimb receiving areas in the anterior lobe or vermis). Also, more generalised

758 suppression of sensory input might result from a contribution of supraspinal, as indicated

759 by our previous findings (Cerminara et al., 2009) in addition to spinal gating as described

760 in the present study.

761   The present study also provides evidence for a strong nociceptive drive to neurons

762 in the MCN. MCN has extensive connections with brainstem structures (Teune et al.,

763 2000), including cells of origin of motor pathways that regulate head movements, posture

764 and proximal limb movements (Ito, 1984). Activation in the vlPAG caused a reduction in

765 the numbers of FLI neurons in response to nociceptor stimulation that was restricted to

766 regions of MCN associated with the A and A2 modules. These regions of MCN have a

767 complex pattern of projections to numerous brainstem structures, including the vestibular

768 nuclei, medial reticular formation and superior colliculus (Teune et al., 2000). Activation

769 of these circuits by noxious peripheral stimuli could therefore result in adjustments in

770 orientation and body posture that might compromise appropriate motor responses in a

771 fearful situation. The present data indicate that activation of the vlPAG depresses

772 nociceptor-evoked response in the MCN and, as a consequence, this could enhance

773 survival by limiting the impact of nociceptive input on the execution of motor responses

774 in fearful situations.

775   *Co-ordinated effects on sensorimotor systems.* In two separate lines of enquiry;

776 one in anesthetised and one in awake animals we provide evidence that the vlPAG has

777 the capacity to co-ordinate effects on motor behaviour together with transmission in

778 SOCPs as assessed by monitoring changes in CFPs to electrical stimulation of the

779 ipsilateral hindlimb. The data are consistent with our previous report in anesthetised rats

780 (Cerminara et al., 2009) i.e. that vlPAG activation causes a reduction in transmission in

781 SOCPs, but the present study extends this to show that this is closely linked to freezing

782 behavior.

783   We have previously reported facilitation of α-motoneuronal activity from vlPAG

784 as measured by an increase in H-reflex excitability (Koutsikou et al., 2014), and have

785 suggested that this effect might contribute to the role of the PAG in freezing, which

786 involves a generalised and sustained increase in muscle tone. Taken together with our

787 current results, in both anesthetised and awake animals, this suggests that localised pools

788 of neurons in the vlPAG simultaneously co-ordinate effects on sensory transmission in

789 SOCPs and on motor outflow. The underlying neural circuits remain to be fully

790 characterised. However, it may be relevant to note that direct connections exist between

791 the vlPAG and the inferior olive (Rutherford et al., 1984; Holstege, 1988; Van Bockstaele

792 et al., 1991; Watson et al., 2013). Such a projection may play a role in gating SOCP

793 transmission, although it should be emphasized that the modulation could occur via other

794 indirect pathways. With regard to vlPAG influence on spinal reflex circuits, our previous

795 studies have shown that this is dependent on a transcerebellar circuit involving vermal

796 lobule VIII (the pyramis, Koutsikou et al., 2014).

797   *Functional Significance.* We suggest that the differential gating of nociceptive

798 cutaneous and proprioceptive information to the cerebellum by the vlPAG, together with

799 the enhancement of motor outflow may contribute to the generation of appropriate motor

800 responses associated with freezing behavior. More specifically, the engagement of co-

801 ordinated influences from the vlPAG promotes a condition where the animal is ready

802 (enhanced proprioceptive input and increased muscle activity, so promoting directed

803 active coping behavior; Walker and Carrive, 2003) and able to escape (less likely to be

804 perturbed by noxious sensory information), thus assisting survival.

805

References

807 Ackerley R, Pardoe J, Apps R (2006) A novel site of synaptic relay for climbing fibre
808   pathways relaying signals from the motor cortex to the cerebellar cortical C1
809   zone. J Physiol 576:503-518.
810 Apps R (1999) Movement-related gating of climbing fibre input to cerebellar cortical
811   zones. Prog Neurobiol 57:537-562.
812 Apps R (2000) Gating of climbing fibre input to cerebellar cortical zones. Prog Brain Res
813   124:201-211.
814 Apps R, Lee S (1999) Gating of transmission in climbing fibre paths to cerebellar cortical
815   C1 and C3 zones in the rostral paramedian lobule during locomotion in the cat. J
816   Physiol 516 (Pt 3):875-883.
817 Apps R, Hartell NA, Armstrong DM (1995) Step phase-related excitability changes in
818   spino-olivocerebellar paths to the c1 and c3 zones in cat cerebellum. J Physiol 483
819   (Pt 3):687-702.
820 Armstrong DM, Harvey RJ (1968) Responses to a spino-olivo-cerebellar pathway in the
821   cat. J Physiol 194:147-168.
822 Armstrong DM, Eccles JC, Harvey RJ, Matthews PB (1968) Responses in the dorsal
823   accessory olive of the cat to stimulation of hind limb afferents. J Physiol 194:125-
824   145.
825 Atkins MJ, Apps R (1997) Somatotopical organisation within the climbing fibre
826   projection to the paramedian lobule and copula pyramidis of the rat cerebellum. J
827   Comp Neurol 389:249-263.
828 Azizi SA, Woodward DJ (1987) Inferior olivary nuclear complex of the rat: morphology
829   and comments on the principles of organization within the olivocerebellar system.
830   J Comp Neurol 263:467-484.
831 Baker MR, Javid M, Edgley SA (2001a) Activation of cerebellar climbing fibres to rat
832   cerebellar posterior lobe from motor cortical output pathways. J Physiol 536:825-
833   839.
834 Baker MR, Javid M, Edgley SA (2001b) Activation of cerebellar climbing fibres to rat
835   cerebellar posterior lobe from motor cortical output pathways. The Journal of
836   physiology 536:825-839.
837 Blanchard RJ, Blanchard DC (1969) Crouching as an index of fear. J Comp Physiol
838   Psychol 67:370-375.
839 Buisseret-Delmas C (1988) Sagittal organization of the olivocerebellonuclear pathway in
840   the rat. I. Connections with the nucleus fastigii and the nucleus vestibularis
841   lateralis. Neuroscience research 5:475-493.
842 Buisseret-Delmas C, Angaut P (1993) The cerebellar olivo-corticonuclear connections in
843   the rat. Prog Neurobiol 40:63-87.

844   Carrive P, Leung P, Harris J, Paxinos G (1997) Conditioned fear to context is associated
845   with increased Fos expression in the caudal ventrolateral region of the midbrain
846   periaqueductal gray. Neuroscience 78:165-177.
847   Cerminara NL, Apps R (2011) Behavioural significance of cerebellar modules.
848   Cerebellum 10:484-494.
849   Cerminara NL, Koutsikou S, Lumb BM, Apps R (2009) The periaqueductal grey
850   modulates sensory input to the cerebellum: a role in coping behaviour? The
851   European journal of neuroscience 29:2197-2206.
852   Chen XY, Wolpaw JR (2005) Ablation of cerebellar nuclei prevents H-reflex down-
853   conditioning in rats. Learning & memory 12:248-254.
854   Chung JM, Kenshalo DR, Jr., Gerhart KD, Willis WD (1979) Excitation of primate
855   spinothalamic neurons by cutaneous C-fiber volleys. J Neurophysiol 42:1354-
856   1369.
857   Eccles JC, Llinas R, Sasaki K (1966) The excitatory synaptic action of climbing fibres on
858   the purinje cells of the cerebellum. J Physiol 182:268-296.
859   Flavell CR, Cerminara NL, Apps R, Lumb BM (2014) Spino-olivary projections in the
860   rat are anatomically separate from postsynaptic dorsal column projections. J
861   Comp Neurol 522:2179-2190.
862   Fuller JH, Schlag JD (1976) Determination of antidromic excitation by the collision test:
863   problems of interpretation. Brain Res 112:283-298.
864   Garwicz M, Ekerot CF, Schouenborg J (1992) Distribution of Cutaneous Nociceptive and
865   Tactile Climbing Fibre Input to Sagittal Zones in Cat Cerebellar Anterior Lobe.
866   Eur J Neurosci 4:289-295.
867   Gozariu M, Roth V, Keime F, Le Bars D, Willer JC (1998) An electrophysiological
868   investigation into the monosynaptic H-reflex in the rat. Brain Res 782:343-347.
869   Hartell NA, Headley PM (1990) Spinal effects of four injectable anaesthetics on
870   nociceptive reflexes in rats: a comparison of electrophysiological and behavioural
871   measurements. Br J Pharmacol 101:563-568.
872   Heinricher MM, Tavares I, Leith JL, Lumb BM (2009) Descending control of
873   nociception: Specificity, recruitment and plasticity. Brain Res Rev 60:214-225.
874   Holstege G (1988) Brainstem-spinal cord projections in the cat, related to control of head
875   and axial movements. Rev Oculomot Res 2:431-470.
876   Hunt SP, Pini A, Evan G (1987) Induction of c-fos-like protein in spinal cord neurons
877   following sensory stimulation. Nature 328:632-634.
878   Ito M (1984) Cerebellum and Neural Control. New York: Raven Press.
879   Ito M (2001) Cerebellar long-term depression: characterization, signal transduction, and
880   functional roles. Physiol Rev 81:1143-1195.
881   Jorntell H, Ekerot C, Garwicz M, Luo XL (2000) Functional organization of climbing
882   fibre projection to the cerebellar anterior lobe of the rat. J Physiol 522 Pt 2:297-
883   309.
884   Kennedy TT, Grimm RJ, Towe AL (1966) The role of cerebral cortex in evoked
885   somatosensory activity in cat cerebellum. Exp Neurol 14:13-32.
886   Koutsikou S, Parry DM, MacMillan FM, Lumb BM (2007) Laminar organization of
887   spinal dorsal horn neurones activated by C- vs. A-heat nociceptors and their
888   descending control from the periaqueductal grey in the rat. The European journal
889   of neuroscience 26:943-952.

890   Koutsikou S, Crook JJ, Earl EV, Leith JL, Watson TC, Lumb BM, Apps R (2014) Neural
891   substrates underlying fear-evoked freezing: the periaqueductal grey-cerebellar
892   link. The Journal of physiology 592:2197-2213.
893   LaFleur BJ, Greevy RA (2009) Introduction to permutation and resampling-based
894   hypothesis tests. Journal of clinical child and adolescent psychology : the official
895   journal for the Society of Clinical Child and Adolescent Psychology, American
896   Psychological Association, Division 53 38:286-294.
897   LeDoux J (2012) Rethinking the emotional brain. Neuron 73:653-676.
898   LeDoux JE, Iwata J, Cicchetti P, Reis DJ (1988) Different projections of the central
899   amygdaloid nucleus mediate autonomic and behavioral correlates of conditioned
900   fear. The Journal of neuroscience : the official journal of the Society for
901   Neuroscience 8:2517-2529.
902   Leith JL, Koutsikou S, Lumb BM, Apps R (2010) Spinal processing of noxious and
903   innocuous cold information: differential modulation by the periaqueductal gray.
904   The Journal of neuroscience : the official journal of the Society for Neuroscience
905   30:4933-4942.
906   Lidierth M, Apps R (1990) Gating in the spino-olivocerebellar pathways to the c1 zone of
907   the cerebellar cortex during locomotion in the cat. J Physiol 430:453-469.
908   Lipski J (1981) Antidromic activation of neurones as an analytic tool in the study of the
909   central nervous system. J Neurosci Methods 4:1-32.
910   Llinas RR (2011) Cerebellar motor learning versus cerebellar motor timing: the climbing
911   fibre story. J Physiol 589:3423-3432.
912   Lovick TA, Bandler R (2005) The organisation of the midbrain periaqueductal grey and
913   the integration of pain behaviours In: The neurobiology of pain (Hunt SP,
914   Koltzenburg M, eds), pp 267-287. Oxford: Oxford UP.
915   Lumb BM (2004) Hypothalamic and midbrain circuitry that distinguishes between
916   escapable and inescapable pain. News Physiol Sci 19:22-26.
917   Mattsson JL, Albee RR, Brandt LM (1984) H-reflex waveform and latency variability in
918   rats. Fundam Appl Toxicol 4:944-948.
919   McMullan S, Lumb BM (2006a) Midbrain control of spinal nociception discriminates
920   between responses evoked by myelinated and unmyelinated heat nociceptors in
921   the rat. Pain 124:59-68.
922   McMullan S, Lumb BM (2006b) Spinal dorsal horn neuronal responses to myelinated
923   versus unmyelinated heat nociceptors and their modulation by activation of the
924   periaqueductal grey in the rat. J Physiol 576:547-556.
925   Menetrey D, Giesler GJ, Jr., Besson JM (1977) An analysis of response properties of
926   spinal cord dorsal horn neurones to nonnoxious and noxious stimuli in the spinal
927   rat. Exp Brain Res 27:15-33.
928   Merrill EG, Ainsworth A (1972) Glass-coated platinum-plated tungsten microelectrodes.
929   Med Biol Eng 10:662-672.
930   Molinari HH, Dostrovsky JO (1987) Functional properties of neurons in the cat gracile
931   nucleus that project to the dorsal accessory olive. Exp Brain Res 69:119-130.
932   Morissette J, Bower JM (1996) Contribution of somatosensory cortex to responses in the
933   rat cerebellar granule cell layer following peripheral tactile stimulation. Exp Brain
934   Res 109:240-250.

935   Oscarsson O (1968) Termination and functional organization of the ventral spino-
936   olivocerebellar path. J Physiol 196:453-478.
937   Oscarsson O, Sjolund B (1977) The ventral spino-olivocerebellar system in the cat. III.
938   Functional characteristics of the five paths. Exp Brain Res 28:505-520.
939   Pardoe J, Apps R (2002) Structure-function relations of two somatotopically
940   corresponding regions of the rat cerebellar cortex: olivo-cortico-nuclear
941   connections. Cerebellum 1:165-184.
942   Pardoe J, Edgley SA, Drew T, Apps R (2004) Changes in excitability of ascending and
943   descending inputs to cerebellar climbing fibers during locomotion. J Neurosci
944   24:2656-2666.
945   Paxinos G, Watson C (2005) The rat brain in stereotaxic coordinates, 2nd Edition.
946   Sydney.
947   Pijpers A, Voogd J, Ruigrok TJ (2005) Topography of olivo-cortico-nuclear modules in
948   the intermediate cerebellum of the rat. J Comp Neurol 492:193-213.
949   Pijpers A, Winkelman BH, Bronsing R, Ruigrok TJ (2008) Selective impairment of the
950   cerebellar C1 module involved in rat hind limb control reduces step-dependent
951   modulation of cutaneous reflexes. J Neurosci 28:2179-2189.
952   Pijpers A, Apps R, Pardoe J, Voogd J, Ruigrok TJ (2006) Precise spatial relationships
953   between mossy fibers and climbing fibers in rat cerebellar cortical zones. J
954   Neurosci 26:12067-12080.
955   Ruigrok TJ, Voogd J (1990) Cerebellar nucleo-olivary projections in the rat: an
956   anterograde tracing study with Phaseolus vulgaris-leucoagglutinin (PHA-L). J
957   Comp Neurol 298:315-333.
958   Ruigrok TJ, Voogd J (2000) Organization of projections from the inferior olive to the
959   cerebellar nuclei in the rat. J Comp Neurol 426:209-228.
960   Rutherford JG, Anderson WA, Gwyn DG (1984) A reevaluation of midbrain and
961   diencephalic projections to the inferior olive in rat with particular reference to the
962   rubro-olivary pathway. J Comp Neurol 229:285-300.
963   Sacchetti B, Scelfo B, Tempia F, Strata P (2004) Long-term synaptic changes induced in
964   the cerebellar cortex by fear conditioning. Neuron 42:973-982.
965   Simpson DA, Headley PM, Lumb BM (2008) Selective inhibition from the anterior
966   hypothalamus of C- versus A-fibre mediated spinal nociception. Pain 136:305-
967   312.
968   Steenland HW, Zhuo M (2009) Neck electromyography is an effective measure of fear
969   behavior. J Neurosci Methods 177:355-360.
970   Szucs P, Luz LL, Lima D, Safronov BV (2010) Local axon collaterals of lamina I
971   projection neurons in the spinal cord of young rats. J Comp Neurol 518:2645-
972   2665.
973   Teune TM, van der Burg J, de Zeeuw CI, Voogd J, Ruigrok TJ (1998) Single Purkinje
974   cell can innervate multiple classes of projection neurons in the cerebellar nuclei of
975   the rat: a light microscopic and ultrastructural triple-tracer study in the rat. J
976   Comp Neurol 392:164-178.
977   Teune TM, van der Burg J, van der Moer J, Voogd J, Ruigrok TJ (2000) Topography of
978   cerebellar nuclear projections to the brain stem in the rat. Prog Brain Res
979   124:141-172.

980   Van Bockstaele EJ, Aston-Jones G, Pieribone VA, Ennis M, Shipley MT (1991)
981   Subregions of the periaqueductal gray topographically innervate the rostral
982   ventral medulla in the rat. J Comp Neurol 309:305-327.
983   Walker P, Carrive P (2003) Role of ventrolateral periaqueductal gray neurons in the
984   behavioral and cardiovascular responses to contextual conditioned fear and
985   poststress recovery. Neuroscience 116:897-912.
986   Waters AJ, Lumb BM (1997) Inhibitory effects evoked from both the lateral and
987   ventrolateral periaqueductal grey are selective for the nociceptive responses of rat
988   dorsal horn neurones. Brain Res 752:239-249.
989   Waters AJ, Lumb BM (2008) Descending control of spinal nociception from the
990   periaqueductal grey distinguishes between neurons with and without C-fibre
991   inputs. Pain 134:32-40.
992   Watson TC, Koutsikou S, Cerminara NL, Flavell CR, Crook JJ, Lumb BM, Apps R
993   (2013) The olivo-cerebellar system and its relationship to survival circuits.
994   Frontiers in neural circuits 7:72.
995   Workman BJ, Lumb BM (1997) Inhibitory effects evoked from the anterior
996   hypothalamus are selective for the nociceptive responses of dorsal horn neurons
997   with high- and low-threshold inputs. J Neurophysiol 77:2831-2835.
998

999   **Figure Legends**

1000   **Figure 1.** Characteristics of spino-olivary projection neurons. *a,* Typical single case

1001   example of antidromic testing, demonstrating (i) the constant latency of the

1002   antidromically-evoked spike (5 consecutive trials superimposed), (ii) ability to follow

1003   high frequency stimulation (200 Hz) and (iii) collision (asterisk) with an orthodromically-

1004   evoked spike. *b,* Mean ± SEM of the thresholds (*n = 5)* for antidromic activation as a

1005   function of the position of the stimulating electrode in the inferior olivary complex (IO).

1006   Zero indicates the location of the stimulating electrode at a depth where the minimum

1007   current was required to evoke an antidromic spike. This location coincided

1008   stereotactically with the IO and was confirmed histologically. *c,* Distribution of the

1009   antidromic activation latencies of all spino-olivary neurons according to receptive field

1010   class, including neurons with unidentified peripheral receptive field (No RF). *d*,

1011   Histological identification of location of stimulation sites in the IO (two sites were not

1012   recovered) plotted on standard transverse maps of the IO (MAO, medial accessory olive;

1013   DAO, dorsal accessory olive; and PO, principal olive; DC, dorsal cap; VLO, ventrolateral

1014   outgrowth). Purple, Class 1; Green, Class 2; Red, Class 3; Blue, Class 4.

1015

1016 **Figure 2.** Ventrolateral PAG stimulation selectively alters responses to different qualities

1017 of sensory input of spino-olivary projection neurons. *a,* Typical example of the response

1018 of a Class 2 neuron to noxious pinch (3.6N): peri-stimulus time histogram (PSTH, spikes

1019 per 1s bin) are shown before (prePAG) and during (PAG) ventrolateral (vl) PAG

1020 chemical excitation. Dotted horizontal line in each of the PSTHs indicates the onset and

1021 duration of the peripheral stimulus. Bar chart shows the average effect of vlPAG

1022 stimulation on all Class 2 neuronal responses to noxious pinch (*n = 7 neurons*) before

1023 (prePAG), during (PAG) and after (postPAG) microinjection of DLH into vlPAG. *b,*

1024 Same as A except example Class 2 neuron response to innocuous pressure (0.5N; *n = 3*

1025 *neurons*). *c,* Same as A except example of Class 3 neuron response to noxious pinch

1026 (3.6N; *n = 6 neurons*). *d,* Same as A except example of Class 4 neuron response to

1027 innocuous ankle joint manipulation (*n = 8 neurons*). All data are expressed as mean ±

1028 SEM of normalized spike counts in response to natural stimuli on the receptive field. **P*

1029 *< 0.05 , **P < 0.01, ***P < 0.001, **** P < 0.0001* using repeated measures ANOVA

1030 followed by Dunnett's post test versus prePAG. *e,* Example of the response of a single

1031 Class 1 neuron to innocuous pressure (0.5N): PSTH as described in *a*. *f,* Standard

1032 transverse maps of the left PAG at 3 rostrocaudal levels to show histological

1033 reconstruction of injection sites in all but 3 cases in which tissue could be recovered. In

1034 every case the site of injection was verified physiologically with a transient drop in blood

1035 pressure in response to microinjection of DLH into vlPAG. Co-ordinates are relative to

1036 bregma (DM, dorsomedial; DL, dorsolateral; L, lateral; VL, ventrolateral). Purple, Class

1037 1; Green, Class 2 (noxious pinch); Green with black outline, Class 2 (noxious pinch &

1038 innocuous pressure); Red, Class 3; Blue, Class 4.

1039

1040 **Figure 3.** Effects of noxious stimulation and vlPAG activation on FLI-expression in the

1041 A and A2 subdivisions of the cerebellar nuclei. *a,* Standard transverse sections of the

1042 right hand cerebellar nuclei showing distribution of FLI neurons for 4 experimental

1043 groups. From left to right: microinjection of (i) saline into vlPAG (*n* = 7), (ii)

1044 microinjection of DLH into vlPAG (*n* = 7), (iii) anesthetic control (*n* = 8), and (iv)

1045 noxious pinch of the snout (*n* = 6). Each individual dot represents one FLI neuron.

1046 Results from all animals in each group are overlaid, *b,* Mean number of FLI neurons per

1047   section in the A and A2 subdivisions for animals in each experimental group. Data are

1048   represented as mean ±SEM. *$P < 0.05$, *post-hoc* permutation t-test with Bonferroni's

1049   correction. *c,* Standard transverse maps of the left PAG at 2 rostrocaudal levels to show

1050   histological reconstruction of injection sites of DLH (filled circles) and saline (open

1051   circles). Abbreviations: no-STx; no stereotaxy involved in experiment (i.e. no nose clamp

1052   or ear bars were used), STx; stereotaxy involved in experiments (i.e. nose clamp and ear

1053   bars were used).

1054

1055   **Figure 4.** Effects of noxious stimulation and vlPAG activation on FLI expression in the

1056   AX subdivision of the cerebellar nuclei and control experiments with nitroprusside. *a,*

1057   Mean number of FLI neurons per section in the AX subdivision of the medial cerebellar

1058   nucleus (MCN) for animals in each experimental group. No statistically significant

1059   differences were observed between groups with microinjection of saline into vlPAG ($n =$

1060   7), microinjection of DLH into vlPAG ($n = 7$), anesthetic control ($n = 8$), and noxious

1061   pinch of the snout ($n = 6$, $P > 0.05$, permutation one-way ANOVA). *b,* Mean number of

1062   FLI neurons per section in different subdivisions of MCN for anesthetic control (Anesth)

1063   and nitroprusside (Nitro) control groups. No significant differences in FLI in the MCN

1064   were observed between animals administered with sodium nitroprusside (n=4) and

1065   anesthetic control animals (n=8, $P > 0.05$, permutation one-way ANOVA).

1066

1067   **Figure 5.** Characterisation of hindlimb evoked cerebellar field potentials (CFPs) in

1068   awake rat. *a,* Superimposition of 3 consecutive field potentials evoked by electrical

1069   stimulation of the ipsilateral hindlimb (1.5x threshold) in an awake rat (stimulus onset

1070   indicated by filled arrowhead). *b,* Sagittal section of cerebellum showing electrode

1071   position (lesion indicated by filled arrowhead) from which recordings shown in (*a*) were

1072   made. *c,* upper two traces: example average field potential waveforms (10 consecutive

1073   trials) recorded simultaneously from two positions shown in the sagittal section of the

1074   cerebellum. Lower trace, simultaneously recorded neck EMG. *d,* Stimulus response curve

1075   for CFPs (red dashed line) and EMG (black dashed line) following ipsilateral hindlimb

1076   stimulation ($n = 7$ rats). Stimulus intensity expressed as multiples of threshold (T)

1077   required to evoke a detectable cerebellar response. *e,* The effect of paired hindlimb

1078   stimulation on the amplitude of the early (black dashed line) and late component (red

1079   dashed line) of evoked CFPs recorded in COP (*n* = 7 rats). *f*, Example CFP (upper trace)

1080   and individual Purkinje cell complex spike (lower trace) evoked by ipsilateral hindlimb

1081   stimulation (indicated by filled arrowhead) recorded from the same position in COP in

1082   one rat. CI, crus I; CII, crus II; COP, copula pyramidis; PML, paramedian lobule.

1083

1084   **Figure 6.** Evidence of modulation in olivocerebellar pathway transmission during

1085   freezing. *a,* In one animal, the excitatory amino acid DLH was injected (100nl, 50mM;

1086   dashed line indicates time of injection) into the vlPAG while recording CFP responses

1087   evoked by ipsilateral hindlimb stimulation. DLH injection resulted in a reduction in CFP

1088   amplitude together with a robust expression of freezing-like behavior (horizontal black

1089   bar indicates period in which the rat spent 95% of time in freezing-like behavior; light

1090   gray bars indicate baseline (55%) and recovery (52%) levels of inactivity, respectively).

1091   *b,* Camera lucida drawing of transverse view of PAG (-8.16mm relative to bregma),

1092   showing location of bilateral injection cannulae (indicated by filled areas). *c,* Group data

1093   from fear conditioning experiments in which the amplitude of evoked CFPs was

1094   measured during periods of spontaneous inactivity (open bar, prior to fear recall) and

1095   during identified freezing epochs (filled bar, following exposure to previously

1096   conditioned stimuli). *** $P < 0.001$, paired t-test; *n* = 5 rats). *d,* EMG amplitude during

1097   the same conditions as in (*c)* (* $P < 0.05$, paired t-test; *n* = 5 rats). dm, dorsomedial PAG;

1098   lat, lateral PAG; dl, dorsolateral PAG; vl, ventrolateral PAG.

1099

1100   **Figure 7.** Activation of vlPAG results in simultaneous, differential modulation of SOCP

1101   transmission and spinal reflex circuits. *a-i,* example climbing fiber field potentials (CFP)

1102   recorded from the surface of the cerebellar cortex (C1 zone of left copula pyramidis) and

1103   *a-ii* examples of averaged M-wave (M) and H-reflex (H) responses recorded from the left

1104   plantaris muscle at the same time as a-i. All responses were evoked by electrical

1105   stimulation of the ipsilateral tibial nerve (<1mA). Each example consists of five

1106   consecutive responses averaged before (prePAG) and during (PAG) vlPAG chemical

1107   excitation with DLH. Arrows indicate onset of the electrical stimulus. *b,* Group data

1108   (mean ± SEM) showing that microinjections of DLH into the vlPAG facilitate the mean

1109   H-reflex amplitude expressed relative to the size of the M-wave (H:M ratio) during

1110   (PAG) vlPAG neuronal activation (open bars; left Y axis; $n = 5$, **$P = 0.0025$, $F(2, 72) =$

1111   10.45, repeated measures ANOVA followed by Dunnett's post test versus prePAG.)

1112   Simultaneously, vlPAG excitation reduces CFP responses evoked by the same electrical

1113   stimulus (hatched bars; right Y axis; $n = 5$, ****$P < 0.0001$, $F(2, 72) = 92.46$, repeated

1114   measures ANOVA followed by Dunnett's post test versus prePAG). *c,* Standard

1115   transverse maps of the left PAG to show location of injection sites of DLH in the vlPAG

1116   (filled circles). Coordinates are relative to bregma (DM, dorsomedial; DL, dorsolateral;

1117   L, lateral; VL, ventrolateral).

a

(i) Constant Latency

(ii) Following Frequency

(iii) Collision

*

0.2mV

10ms

b

c

d

Caudal

DMCG
DAO-vf
MAO-rp
PO-vl
PO-dl

MAO-C
MAO-B
MAO-A

VLO
DAO-df

DC
MAO-nβ

Rostral

500μm

a: Class 2 (Noxious pinch)

prePAG   PAG

150 spikes/s — 0

20s
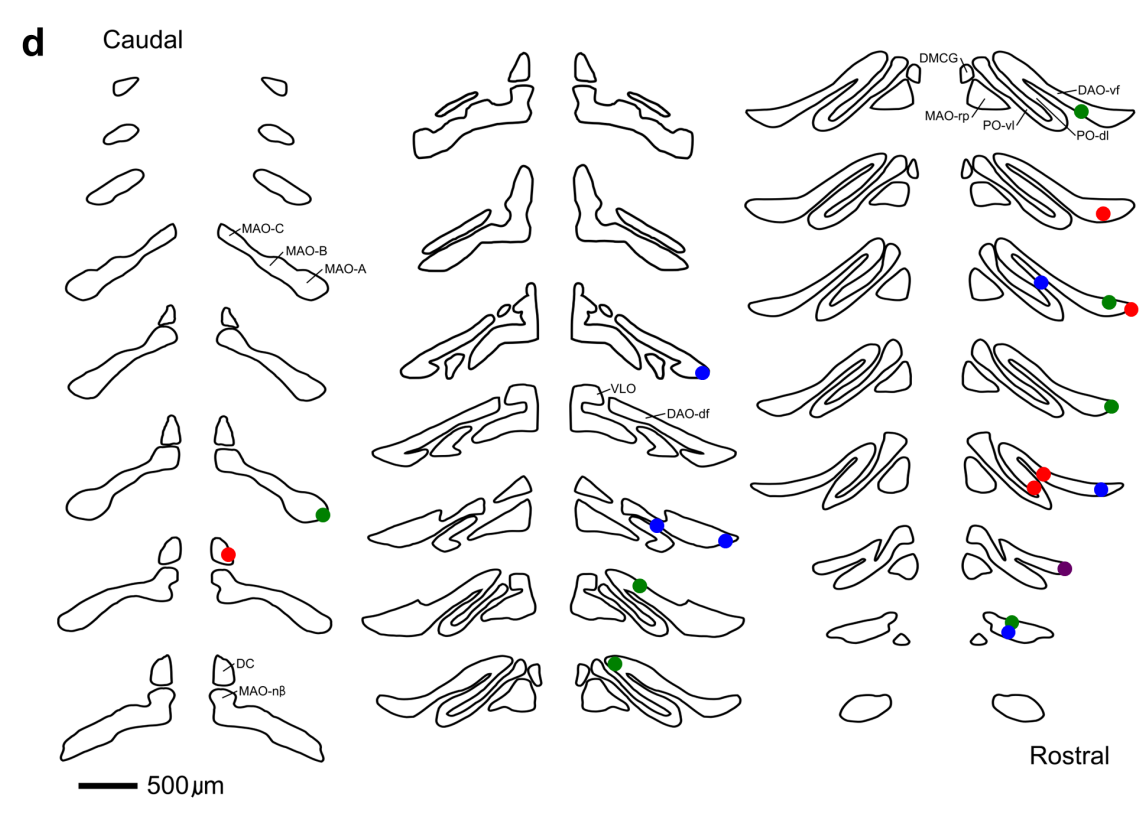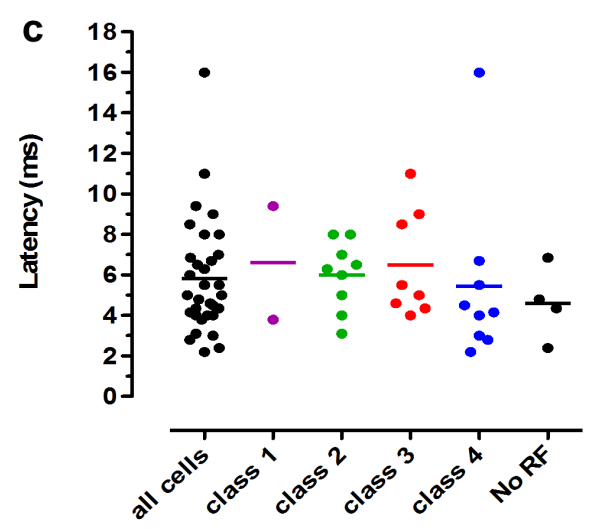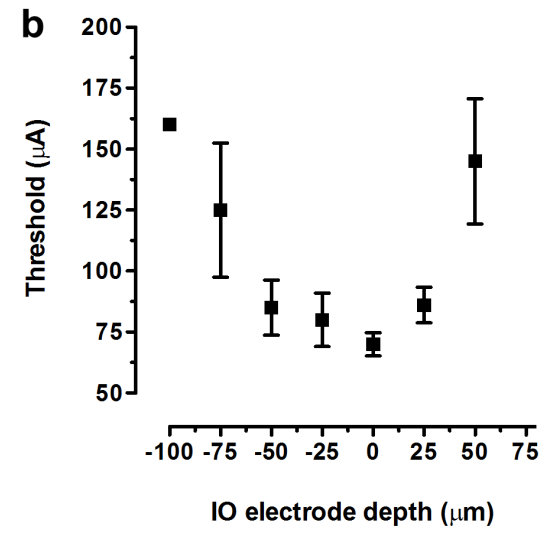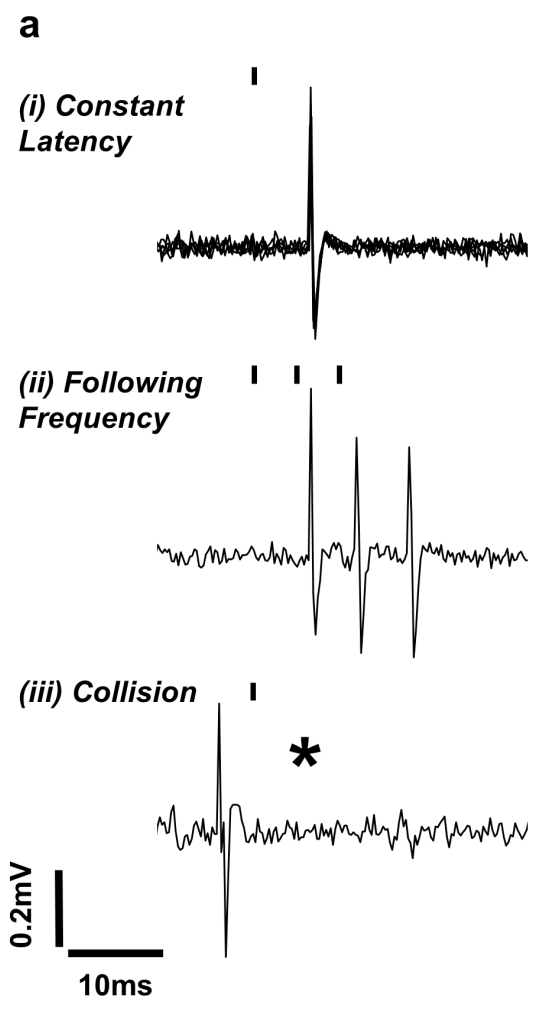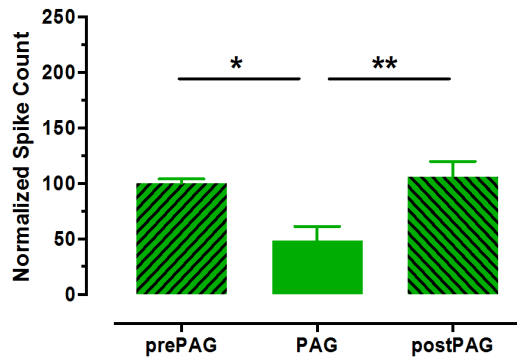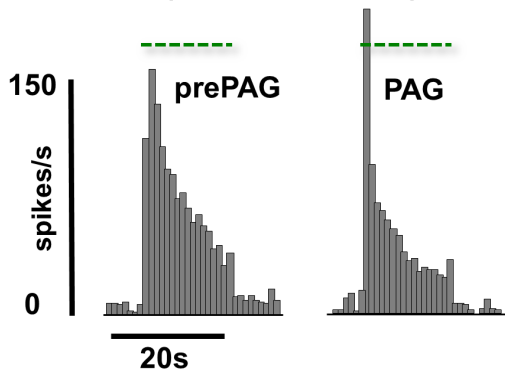
b: Class 2 (Innocuous pressure)

70 spikes/s — 0

10s

c: Class 3 (Noxious pinch)

15 spikes/s — 0

15s

d: Class 4 (Proprioceptive)

20 spikes/s — 0

10s
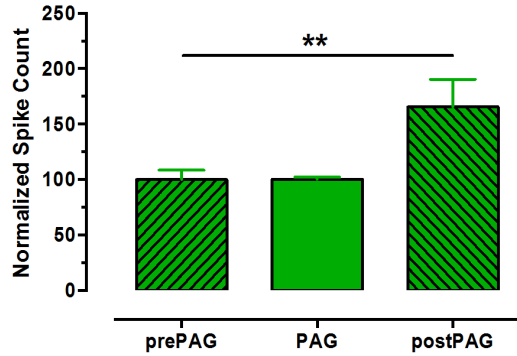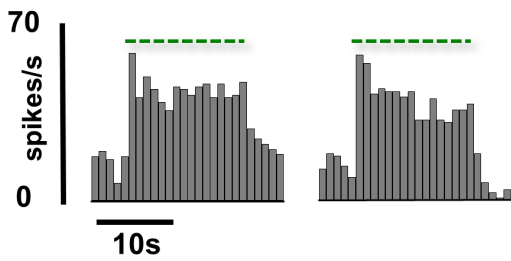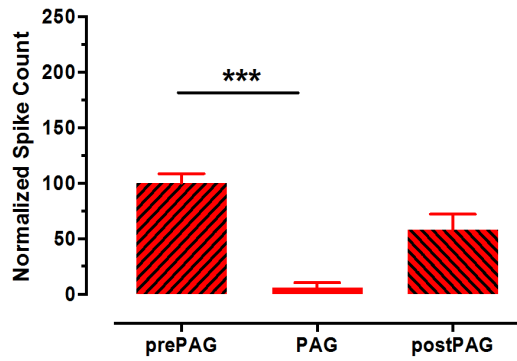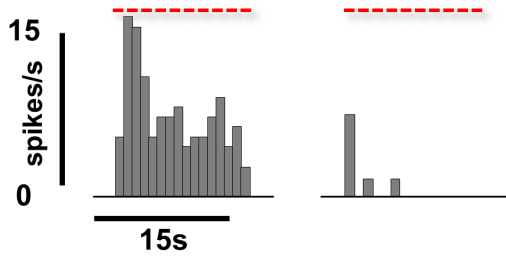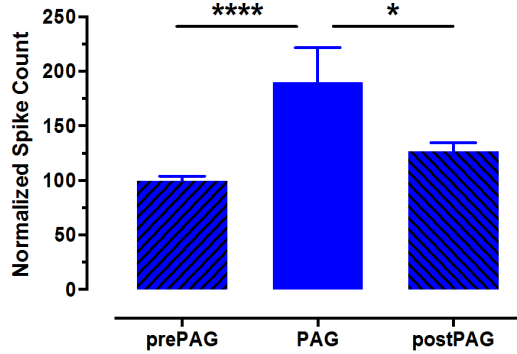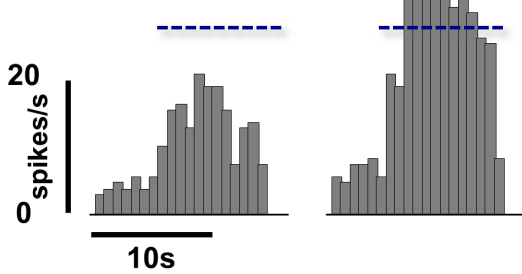
e: Class 1 (Innocuous pressure)

4 spikes/s — 0

5s

f

DL   DM

L

VL

-7.56   -7.92   -8.28

Normalized Spike Count

prePAG   PAG   postPAG

*   **

***

****   *

a

(i) Saline (STx) (ii) DLH (STx) (iii) Anesthetic (no-STx) (iv) Noxious pinch (no-STx)

Caudal

A2
A
AX

1.0mm

Rostral

b

*
*
p=0.057

*
*

Mean number of FLI positive neurons per section

25
20
15
10
5
0

Saline (STx) DLH (STx) Anest. (no-STx) Pinch (no-STx)

A module

Saline (STx) DLH (STx) Anest. (no-STx) Pinch (no-STx)

A2 module

c

DM
DL
L
VL

-7.92

DM
L
VL

-8.28

a

0.5mV

10ms

b

CI
CII
PML
COP

1mm

c

CI
CII
①
PML
②
COP

1mm

①
②
EMG

0.5mV

10ms

d

Peak-to-trough amplitude
(% of maximum response)

75

50

1.0   1.5   2.0   2.5   3.0
Stimulus intensity (X threshold)

e

Response (% of control)

100

80

60

30   60   90   120
Inter pulse interval (ms)

f

0.3 mV

20ms

a

b

c

d

a-i

prePAG

CFP

PAG

0.1mV

10ms

a-ii

prePAG

M   H

PAG

1mV

5ms

b

H:M ratio

Cerebellar field (mV)

**

****

****

prePAG   PAG   postPAG

☐ H:M ratio
▨ Cerebellar field (mV)

c

DL   DM

L

VL

-7.56

DL   DM

L

VL

-7.92

DM

L

VL

-8.28